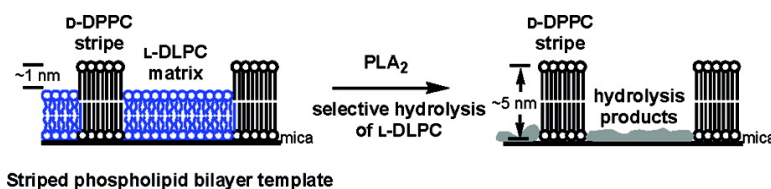


Enzymatic Lithography of Phospholipid Bilayer Films by Stereoselective Hydrolysis

Patricia Moraille, and Antonella Badia

J. Am. Chem. Soc., **2005**, 127 (18), 6546-6547 • DOI: 10.1021/ja0511669 • Publication Date (Web): 16 April 2005

Downloaded from <http://pubs.acs.org> on March 25, 2009



More About This Article

Additional resources and features associated with this article are available within the HTML version:

- Supporting Information
- Access to high resolution figures
- Links to articles and content related to this article
- Copyright permission to reproduce figures and/or text from this article

[View the Full Text HTML](#)



Enzymatic Lithography of Phospholipid Bilayer Films by Stereoselective Hydrolysis

Patricia Moraille and Antonella Badia*

Department of Chemistry and Centre for Self-Assembled Chemical Structures, Université de Montréal,
C.P. 6128, succursale Centre-ville, Montréal, QC H3C 3J7 Canada

Received February 23, 2005; E-mail: antonella.badia@umontreal.ca

Enzymes are appealing nanolithography tools due to their high specificity and efficiency at catalyzing chemical reactions under mild conditions in aqueous medium. Recent studies have demonstrated the feasibility of using enzymes to create specific nanoscale motifs in organic thin film surfaces.¹ Directing and confining the enzyme reaction to defined regions of a surface remains, however, the fundamental challenge in enzyme-promoted lithography. The main strategy adopted to date is to use the direct-writing capability of scanning probe microscopy and enzyme-modified or -coated probes to direct the enzyme toward a desired location of a homogeneous film surface.^{1b-d} Alternative approaches that do not require proximal probes¹ to localize the enzymatic action must be explored to evaluate the scope and versatility of enzyme lithography.

We have investigated the possibility of spatially directing a stereospecific lipolytic enzyme reaction using surface patterns of the biologically active and inactive enantiomers of the lipid substrate. We used phospholipase A₂ (PLA₂), an interfacially active, calcium-dependent enzyme which catalyzes cleavage of the *sn*-2 ester linkage of glycerophospholipids, yielding fatty acid and lysophospholipid.² The natural L lipid form is hydrolyzed; PLA₂ binds but does not cleave the physicochemically identical D form.³ Atomic force microscopy (AFM) studies of the degradation of one-component, supported planar bilayers of solid-condensed L- α -diacylphosphatidylcholines (di-C_nPCs) have shown that enzymatic hydrolysis starts at hole defects (i.e., exposed lipid cleavage sites), and that PLA₂ degrades both top and bottom layers.⁴ We report herein the *stereoselective* PLA₂ hydrolysis of nanoscale stripe patterns in bilayer films consisting of the L and D isomers of di-C₁₂PC (DLPC) and di-C₁₆PC (DPPC).

Bilayers, consisting of condensed or solid-like DPPC stripes in a fluid DLPC matrix, were prepared by successive Langmuir-Blodgett transfer of two phase-separated DPPC/DLPC (1:3) monolayers from the air/water interface to mica at a surface pressure of 25 mN/m, as previously described.⁵ The resulting pattern results from the superposition of the condensed DPPC stripe domains and fluid DLPC phases present in both layers (Figure 1), as revealed by detergent extraction of the fluid phase from these films⁵ and visualized by near-field scanning optical microscopy⁶. Structural characterization of the striped bilayer and its formation mechanism have been reported elsewhere.⁵ By using combinations of the L, D, and DL (racemic) forms of DPPC and DLPC, we have generated novel membrane templates with *built-in* stereochemical control over the PLA₂ activity.

Each of the enantiomer combinations exhibited the same bilayer pattern structure as the one shown in Figure 2A for D-DPPC/DL-DLPC. Parallel stripes of a thicker DPPC phase are observed; these are ~ 1.1 nm higher than the surrounding matrix^{5,6} and occupy $18 \pm 5\%$ of the total surface area. Regions of narrower broken stripes (width ≈ 130 – 190 nm) are dispersed among areas of wider continuous lines (width ≈ 200 – 300 nm).^{5,7} Bilayer-deep holes,

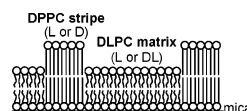


Figure 1. Schematic of the solid-supported DPPC/DLPC bilayer template.

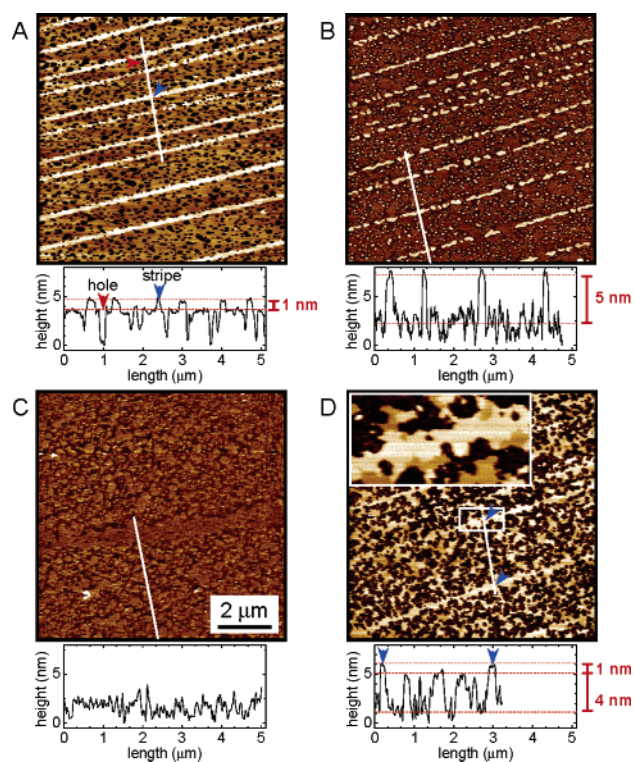


Figure 2. Tapping mode AFM images ($10 \times 10 \mu\text{m}^2$) and height profiles of mica-supported bilayers in aqueous medium. (A) Intact D-DPPC/DL-DLPC. After PLA₂-catalyzed lipid hydrolysis (38 nM PLA₂, 0.7 mM CaCl₂, pH ≈ 8.8): (B) D-DPPC/L-DLPC, (C) L-DPPC/L-DLPC, and (D) D-DPPC/DL-DLPC (inset: $1.8 \times 0.9 \mu\text{m}^2$ magnification).

originating from phospholipid desorption to the air/water interface during transfer of the second monolayer,⁸ are present in the surrounding fluid DLPC phase (hole depth ≈ 4 nm) and along the edges of the DPPC stripes.⁵ These striped bilayers are excellent spatial patterns to test the lithographic performance of PLA₂ due to their regularity, biomimetic interlayer coupling, length scale, and the presence of hole defects and domain boundaries that are known enzyme activation sites⁹.

Figure 2B shows a D-DPPC/L-DLPC bilayer after PLA₂-catalyzed phospholipid hydrolysis. PLA₂ degrades the L-DLPC matrix but not the D-DPPC stripes.¹⁰ The stripes are now an average of ~ 4.7 nm higher than the surrounding phase, which consists predominantly of insoluble aggregates of the hydrolysis products.^{4a,b,d} The non-

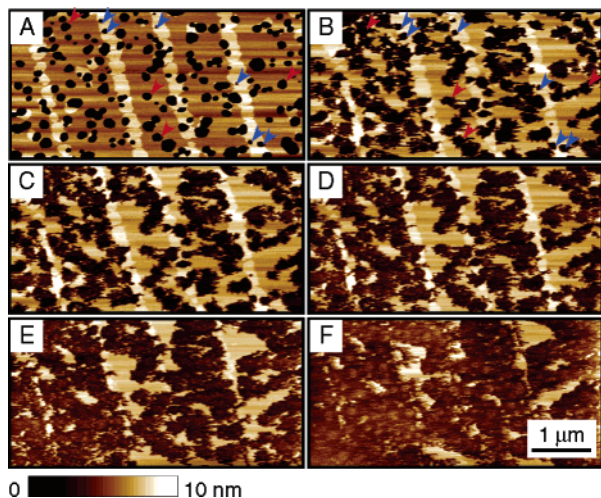


Figure 3. Tapping mode AFM images ($5 \times 2.5 \mu\text{m}^2$) of the PLA₂ hydrolysis of L-DPPC/DL-DLPC. (A) Intact bilayer. (B) 1.43 min, (C) 4.29 min, (D) 7.15 min, (E) 12.87 min, and (F) 21.45 min after PLA₂ addition to the fluid cell (38 nM PLA₂, 0.7 mM CaCl₂, pH \approx 8.8). Times specified correspond to the middle of each image. Arrows: holes in the fluid DLPC (red) and condensed DPPC (blue) phases.

hydrolyzed stripes (width \approx 110–175 nm) exhibit curved edges due to the numerous holes that decorate the stripe edges in the intact bilayer. Circular domains, 50–120 nm in diameter and of the same height as the nonhydrolyzed stripes, are dispersed in the interstripe phase. These nanoscopic structures, whose presence is revealed by PLA₂ hydrolysis of the surrounding L-DLPC, are likely D-DPPC domains that fail to associate or align into stripes at the three phase contact line during film transfer^{5,7} and, therefore, remain in the fluid DLPC matrix.

To establish that the selective hydrolysis of the DLPC matrix of D-DPPC/L-DLPC is due to the stereospecific enzyme activity, rather than the different phase states¹¹ of the DPPC stripes versus the DLPC matrix, L-DPPC/L-DLPC and D-DPPC/DL-DLPC bilayers were also treated with PLA₂.¹² The L-DPPC/L-DLPC stripe pattern (Figure 2C) is completely degraded by PLA₂; only product aggregates remain on the mica surface. This clearly demonstrates that PLA₂ hydrolyzes both the condensed and fluid phases of the L isomer-containing bilayer. In the case of D-DPPC/DL-DLPC (Figure 2D), the D-DPPC stripes of the bilayer are discernible after PLA₂ hydrolysis. The surrounding DL-DLPC matrix is, however, only partially degraded by the enzyme due to competitive inhibition of PLA₂ by D-DLPC.³ This is evident in the two topographic levels (height difference of \sim 1 nm) exhibited by the lipid-covered areas (Figure 2D, inset). The above comparisons thus establish the stereoselective nature of the bilayer degradation. The surface coverage of the remaining or nonhydrolyzed lipid domains (value in parentheses) is related to the amount of D isomer, DPPC or DLPC, present in the film: D-DPPC/DL-DLPC ($35 \pm 2\%$) > D-DPPC/L-DLPC ($18 \pm 2\%$) > L-DPPC/L-DLPC (0%).¹³ Overall, these results indicate that the PLA₂-catalyzed degradation of the stripe pattern is determined by the stereochemical lipid configuration in the different phases.

The unique phase-separated and stereochemically differentiated nature of the membrane template allowed us to compare the effect of the lipid phase state versus the presence of nonhydrolyzable D isomer on the PLA₂ activity. Figure 3 presents a time sequence for the PLA₂ hydrolysis of phospholipids in an L-DPPC/DL-DLPC

bilayer. PLA₂ was added to the AFM fluid cell at the top of Figure 3B. Significant bilayer degradation is observed within the time frame (2.86 min) of the first image (Figure 3B). PLA₂ simultaneously attacks the holes in the condensed DPPC stripes and fluid DLPC matrix (arrows), despite the presence of D isomer in the DLPC phase. Numerous channels extend from the widening holes as the enzyme forges across the lipid bilayer (Figure 3B–D).^{4a,c} Degradation of the more ordered DPPC stripes appears to proceed more slowly than the fluid DLPC phase (Figure 3B–D). When L-DLPC was used instead of DL-DLPC, hydrolysis of the fluid phase proceeded too rapidly to be followed by AFM.¹¹ After a time lapse of \sim 23 min (Figure 3F), the condensed L-DPPC stripes are almost completely degraded by the enzyme, while the surrounding fluid DL-DLPC phase is only partly hydrolyzed.¹³ Although we have used the commercially available DL-DLPC, the results indicate that for D-DLPC, parallel grooves in a DLPC bilayer would be obtained after hydrolysis of L-DPPC/D-DLPC.¹²

In summary, we have demonstrated a proof-of-concept of the selective enzymatic modification of stereochemically differentiated lipid bilayers. Compared to proximal probe-directed enzyme lithography¹, the stereochemically directed enzyme lithography reported here allows the parallel patterning of large surface areas. Given that many enzymes are stereospecific, stereoselective enzymatic transformations (subtractive or additive) are potentially useful tools to structure biomimetic films.

Acknowledgment. This research was supported by NSERC, Research Corporation, FQRNT, and CFI.

Supporting Information Available: Materials and Methods. This material is available free of charge via the Internet at <http://pubs.acs.org>.

References

- (1) (a) Clausen-Schaumann, H.; Grandbois, M.; Gaub, H. E. *Adv. Mater.* **1998**, *10*, 949–952. (b) Hyun, J.; Kim, J.; Craig, S. L.; Chilkoti, A. *J. Am. Chem. Soc.* **2004**, *126*, 4770–4771. (c) Ionescu, R. E.; Marks, R. S.; Gheber, L. A. *Nano Lett.* **2003**, *3*, 1639–1642. (d) Takeda, S.; Nakamura, C.; Miyamoto, C.; Nakamura, N.; Kageshima, M.; Tokumoto, H.; Miyake, J. *Nano Lett.* **2003**, *3*, 1471–1474. (e) Jang, C.-H.; Stevens, B. D.; Carlier, P. R.; Calter, M. A.; Ducker, W. A. *J. Am. Chem. Soc.* **2002**, *124*, 12114–12115. (f) Jang, C.-H.; Stevens, B. D.; Phillips, R.; Calter, M. A.; Ducker, W. A. *Nano Lett.* **2003**, *3*, 691–694.
- (2) Six, D. A.; Dennis, E. A. *Biochim. Biophys. Acta* **2000**, *1488*, 1–19.
- (3) (a) van Deenen, L. L. M.; de Haas, G. H. *Biochim. Biophys. Acta* **1963**, *70*, 538–553. (b) Bensen, P. P. M.; de Haas, G. H.; Pieterse, W. A.; Van Deenen, L. L. M. *Biochim. Biophys. Acta* **1972**, *270*, 364–382. (c) Upreti, G. C.; Rainer, S.; Jain, M. K. *J. Membrane Biol.* **1980**, *55*, 97–112.
- (4) (a) Grandbois, M.; Clausen-Schaumann, H.; Gaub, H. *Biophys. J.* **1998**, *74*, 2398–2404. (b) Kaasgaard, T.; Ipsen, J. H.; Mouritsen, O. G.; Jørgensen, K. *Probe Microscopy* **2001**, *2*, 169–175. (c) Nielsen, L. K.; Risbo, J.; Callisen, T. H.; Bjørnholm, T. *Biochim. Biophys. Acta* **1999**, *1420*, 266–271. (d) Leidy, C.; Mouritsen, O. G.; Jørgensen, K.; Peters, G. H. *Biophys. J.* **2004**, *87*, 408–418.
- (5) Moraille, P.; Badia, A. *Langmuir* **2003**, *19*, 8041–8049.
- (6) Ianoul, A.; Burgos, P.; Lu, Z.; Taylor, R. S.; Johnston, L. J. *Langmuir* **2003**, *19*, 9246–9254.
- (7) Moraille, P.; Badia, A. *Langmuir* **2002**, *18*, 4414–4419.
- (8) Bassereau, P.; Pincet, F. *Langmuir* **1997**, *13*, 7003–7007.
- (9) Jørgensen, K.; Davidsen, J.; Mouritsen, O. G. *FEBS Lett.* **2002**, *531*, 23–27.
- (10) The broken character of the D-DPPC stripes is not due to PLA₂ processing but reflects the imperfect nature of the initial stripe pattern.
- (11) Sanchez, S. A.; Bagatolli, L. A.; Gratton, E.; Hazlett, T. L. *Biophys. J.* **2002**, *82*, 2232–2243.
- (12) An obvious combination for enzyme lithography is L-DPPC/D-DLPC. Only the L and DL forms of DLPC are commercially available. We are currently preparing D-DLPC via PLA₂ hydrolysis of DL-DLPC.
- (13) AFM image analysis consistently shows $<$ 50% remaining lipid in the DL-DLPC phase (after accounting for the initial hole defect coverage of \sim 25%). More detailed studies are underway to examine the enzymatic hydrolysis of solid-condensed and fluid racemic phospholipid bilayers.

JA0511669